ARTICLE IN PRESS

Physica D ▮ (▮▮▮▮) ▮▮▮–▮▮▮

Contents lists available at ScienceDirect

Physica D

journal homepage: www.elsevier.com/locate/physd

Parametric resonance and Hopf bifurcation analysis for a MEMS resonator

Cas van der Avoort [a], Rein van der Hout [b,*], Joost Hulshof [b]

[a] NXP Semiconductors Research, Prof. Holstlaan 4, NL-5656 AA, Eindhoven, The Netherlands

[b] VU University, Faculty of Science, De Boelelaan 1081 A, 1081 HV Amsterdam, The Netherlands

ARTICLE INFO

Article history:
Received 18 January 2010
Received in revised form
24 December 2010
Accepted 7 January 2011
Available online xxxx
Communicated by G. Stepan

Keywords:
MEMS resonator
Clipping
Beating
Hopf bifurcation

ABSTRACT

We study the response of a MEMS resonator, driven in an in-plane length-extensional mode of excitation. It is observed that the amplitude of the resulting vibration has an upper bound, i.e., the response shows saturation. We present a model for this phenomenon, incorporating interaction with a bending mode. We show that this model accurately describes the observed phenomena. The in-plane ("trivial") mode is shown to be stable up to a critical value of the amplitude of the excitation. At this value, a new "bending" branch of solutions bifurcates. For appropriate values of the parameters, a subsequent Hopf bifurcation causes a beating phenomenon, in accordance with experimental observations.

1. Introduction; experiments and observations

For various designs of extensional MEMS resonators, fabricated in SOI (Silicon-on-Insulator, thin Si-wafers), certain driving conditions are observed to cause the response to show saturation, without any evidence of physical obstruction. Next to this, sometimes typical beating patterns are observed. These phenomena may occur at very low physical vibration amplitudes, severely limiting the power handling of the device. In this paper we develop a model, on the basis of which we are able to reproduce accurately the behaviour of our resonators by simulation. A full analysis of the model being too complicated, we construct a simplified model by the method of averaging. On the basis of this simplified model, we show that saturation may be explained by the presence of an out-of-plane oscillation mode, which exchanges energy with the "standard" mode; beating phenomena are explained by the occurrence of Hopf bifurcations in the dynamical system containing this out-of-plane mode.

MEMS resonators are currently being developed as an alternative for quartz crystals as frequency references for electronics [1]. Using standard techniques in semiconductor technology, extensional resonators with large piezo-resistive electrical signal output can be produced [2]. The large-signal behaviour of these devices has been studied frequently, as the maximum physical vibration amplitude of such resonators is poor in some cases. Although non-linear stiffness terms were subject of most studies, a more severe limiting mechanism was identified recently [3]. As stated in the introduction, parametric oscillations are the basis of instability, be it that we focus on instability of *un-intended modes of vibration*. Studies of parametric excitation of MEMS resonators have been presented in the literature [4]. MEMS literature on auto-parametric resonance exists as well [5], but more specifically this literature relates to spontaneous oscillations resulting from a constant (optical) power supply. Auto-parametric coupling of vibrations, as studied in the present paper, is also described as a useful feature for signal mixing [6].

The excitation of unwanted modes in a resonator driven over a defined threshold amplitude is common in the literature and more general than the MEMS topic. As early as in 1951 Weidenhammer [7] described the phenomenon of exciting bending vibrations by periodically compressing a rod longitudinally. Such a rod was extensively studied in a lab experiment by Iwatsubo [8], who also reported the occurrence of unstable amplitudes of the coupled vibrations present in the mechanical system. We present in the current paper how these unstable amplitudes can be described by the occurrence of a Hopf bifurcation. More general than the pure 2:1-condition for auto-parametric resonances would be *combination resonance*. Macroscopic experiments on dynamical systems with many modes of vibration were carried out by Cartmell [9] and modeled by Nayfeh [10]. The general conditions for combination resonance apply to a MEMS resonator as well, but for simplicity we limit our analysis to the special case of internal 2:1-resonance.

Fig. 1 shows two measurements of the same device, at different driving power levels. These experimental results show the in-plane response of a typical MEMS resonator (to be referred to as

* Corresponding author. Tel.: +31 26 3336506.
E-mail address: rvdhout@few.vu.nl (R. van der Hout).

0167-2789/$ – see front matter © 2011 Elsevier B.V. All rights reserved.
doi:10.1016/j.physd.2011.01.004

Please cite this article in press as: C. van der Avoort, et al., Parametric resonance and Hopf bifurcation analysis for a MEMS resonator, Physica D (2011), doi:10.1016/j.physd.2011.01.004

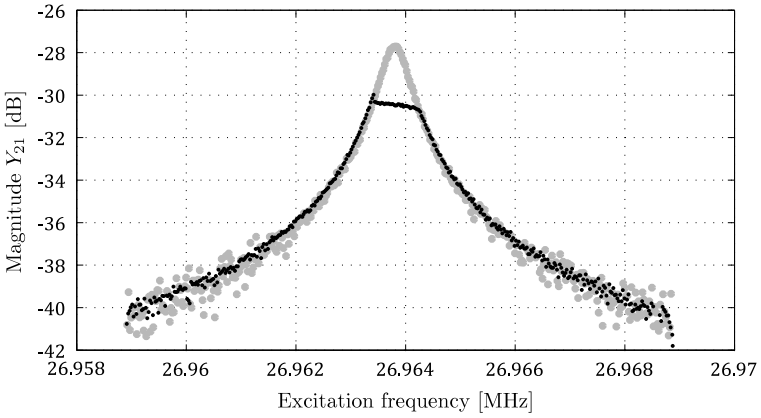

Fig. 1. Two measurements of the same device. **In grey discs**: regular electrical response, plotted as absolute value of transconductance (Y_{21}) versus excitation frequency. The output signal relates to the mechanical motion. **In black dots**: distorted electrical response, obtained by increasing the input power to the resonator. Since the measurement returns a transfer function, the increased input power only shows in the reduced noise.

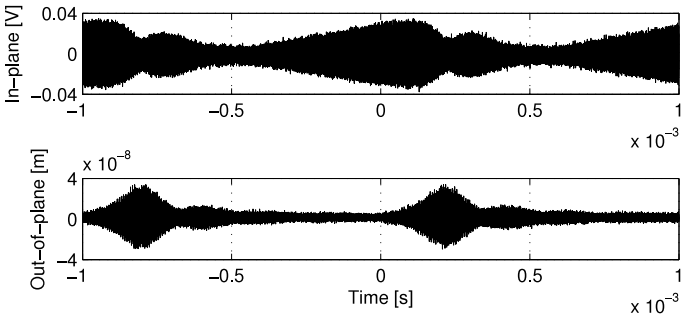

Fig. 2. Example of observed beating in measured time-dependent data for a different resonator. The data for out-of-plane motion have been taken using a Polytec vibrometer, while the in-plane motion was measured directly as an electrical signal. The in-plane signal corresponds to the electrically measured extensional vibration at about 56 MHz. The out-of-plane signal is the optically measured displacement, which modulates at a different frequency. From the complementary amplitudes of the envelopes around the quickly modulating signals, it is clear that the two modes of vibration exchange energy.
Source: Figure by courtesy of K.L. Phan.

a rod) to an in-plane excitation. This excitation is an attractive electrostatic force, modulated around a positive (tension) value. It is to be expected that the mechanical response is maximal in case of resonance, which was the experimental situation. In Fig. 1, at low power a regular mechanical resonance is observed when sweeping the frequency of the modulation of the force. In contrast, Fig. 1 shows saturation when the power or modulation depth is increased. In this paper, we shall address the clipping situation. We shall, on the basis of first principles, show that clipping phenomena can be explained by interaction of the primary trivial extensional mode with other response modes, in this case a specific bending mode. Our analysis also fully explains the occurrence of beating phenomena, which are clearly observable under appropriate conditions, see Fig. 2.

2. Equations of motion; bifurcation of out-of-plane mode

In order to derive a system of equations of motion for our rod, we make the simplifying assumption that any motion of the rod can be decomposed into two modes, vs.

1. the extensional mode $u(x,t) = p(t)\phi(x)$, where ϕ is the first eigenfunction of the operator $\phi \to \phi''$ under the boundary conditions $\phi(0) = \phi'(L) = 0$, and
2. a bending mode $w(x,t) = q(t)\theta(x)$, satisfying $\theta(0) = \theta'(0) = \theta''(L) = \theta'''(L) = 0$, with θ an appropriate eigenfunction (that is, with the first eigenfrequency that is susceptible to resonance to the first eigenfrequency of the extensional mode) of $\theta \to \theta^{(iv)}$.

The equations of motion follow from the Euler–Lagrange equation [11]

$$\frac{\mathrm{d}}{\mathrm{d}t}\left(\frac{\partial T}{\partial \dot{\mathbf{p}}}\right) - \frac{\partial T}{\partial \mathbf{p}} + \frac{\partial V}{\partial \mathbf{p}} = \mathbf{F}, \quad \text{with } \mathbf{p} = \begin{Bmatrix} p(t) \\ q(t) \end{Bmatrix}, \tag{1}$$

where the forces in $\mathbf{F}$ are the electrostatic force for the in-plane mode and zero for the out-of-plane mode. The translation from continuous body motion to modal coordinates stems from the modal expansion theorem [11], according to which

$$\begin{aligned} u(x,t) &= p(t)\theta(x) \\ w(x,t) &= q(t)\phi(x). \end{aligned} \tag{2}$$

The kinetic energy is denoted as

$$\begin{aligned} T &= \frac{1}{2}\rho A \int_0^L \left(\dot{u}^2 + \dot{w}^2\right) \mathrm{d}x \\ &= \frac{1}{2}\rho A \int_0^L \left[\dot{p}^2\theta(x)^2 + \dot{q}^2\phi(x)^2\right] \mathrm{d}x. \end{aligned} \tag{3}$$

It should be noted that the integration over scalar products of mode shapes mainly results in constants and for the motion we are interested in the time-dependent behaviour of the modal coordinates. Hence we write

$$T = \frac{1}{2}\rho A\dot{p}^2 \int \theta^2 \mathrm{d}x + \frac{1}{2}\rho A\dot{q}^2 \int \phi^2 \mathrm{d}x. \tag{4}$$

Associated with u and w we have the local strain, which to first order reads [12]

$$\epsilon = \frac{\partial u}{\partial x} - z\frac{\partial^2 w}{\partial x^2} + \frac{1}{2}\left(\frac{\partial w}{\partial x}\right)^2. \tag{5}$$

Please cite this article in press as: C. van der Avoort, et al., Parametric resonance and Hopf bifurcation analysis for a MEMS resonator, Physica D (2011), doi:10.1016/j.physd.2011.01.004

The definition in Eq. (5) will turn out to be the basis of interaction between the two modes of vibration. The third term is found in expressions for large deformation as applicable to buckling problems. It can also be considered as the term that defines the potential energy of a string under tension. It assumes length extension in order to accommodate for a bending displacement, which in turn does not need to be a large deformation at all. The total potential energy is expressed as

$$V = \frac{1}{2}Eb\int_{-h/2}^{h/2}\int_0^L \epsilon^2 \mathrm{d}x\mathrm{d}z, \tag{6}$$

where beam width b is used instead of area A, as integration over thickness has to take place. Inserting the modal expansion equation (2) and the definition of strain equation (5), we find the potential energy

$$V = \frac{1}{2}EA\left[p^2\int\theta'^2\mathrm{d}x + pq^2\int\theta'\phi'^2\mathrm{d}x + \frac{1}{4}q^4\int\phi'^4\mathrm{d}x\right] + \frac{1}{2}EI\left[q^2\int\phi''^2\mathrm{d}x\right], \tag{7}$$

in which area $A = bh$ and the second moment of area $I = \frac{1}{12}bh^3$ are based on the cross-sectional dimensions.

To construct the equations of motion the expressions for T and V can be inserted in the Lagrange equation, Eq. (1). The kinetic energy T does not depend on the position of any of the coordinates and $\partial T/\partial\mathbf{p}$ is zero. Further we see that

$$\frac{\mathrm{d}}{\mathrm{d}t}\left(\frac{\partial T}{\partial\dot{\mathbf{p}}}\right) = \rho A\begin{Bmatrix}\ddot{p}\int\theta^2\mathrm{d}x\\ \ddot{q}\int\phi^2\mathrm{d}x\end{Bmatrix}, \tag{8}$$

where the integrals are simplified and express the integration from 0 to L and θ and ϕ are the normalized displacement functions satisfying $\theta(L) = \phi(L) = 1$. For the potential energy we find

$$\frac{\partial V}{\partial\mathbf{p}} = \frac{1}{2}\begin{Bmatrix}EA\left(2p\int\theta'^2\mathrm{d}x + q^2\int\theta'\phi'^2\mathrm{d}x\right)\\ EA\left(2pq\int\theta'\phi'^2\mathrm{d}x + q^3\int\phi'^4\mathrm{d}x\right)\\ \quad + EI2q\int\phi''^2\mathrm{d}x\end{Bmatrix}. \tag{9}$$

The mode shapes $\phi(x)$ and $\theta(x)$ lead to scalar values for the inner products, rendering them as purely geometrical factors.

We combine Eqs. (1), (8) and (9) and write the equations of motion as

$$\begin{aligned}\ddot{p} + {\omega_1}^2 p &= -d_1q^2 - \gamma_1\dot{p} - G\cos(\Omega t)\\ \ddot{q} + {\omega_2}^2 q &= -d_2pq - \gamma_2\dot{q} - d_3q^3,\end{aligned} \tag{10}$$

where the constants relate to the shape functions as

$${\omega_1}^2 = \frac{E}{\rho}\frac{\int\theta'^2\mathrm{d}x}{\int\theta^2\mathrm{d}x}, \qquad {\omega_2}^2 = \frac{EI}{\rho A}\frac{\int\phi''^2\mathrm{d}x}{\int\phi^2\mathrm{d}x}, \tag{11}$$

and

$$d_1 = \frac{E}{2\rho}\frac{\int\theta'\phi'^2\mathrm{d}x}{\int\theta^2\mathrm{d}x}, \qquad d_2 = \frac{E}{\rho}\frac{\int\theta'\phi'^2\mathrm{d}x}{\int\phi^2\mathrm{d}x}, \qquad d_3 = \frac{E}{2\rho}\frac{\int\phi'^4\mathrm{d}x}{\int\phi^2\mathrm{d}x}. \tag{12}$$

We have three different frequencies playing a role here, where ω_1 is the small-amplitude eigenfrequency of the in-plane mode, ω_2 is the eigenfrequency of the unwanted out-of-plane mode and Ω is the forcing frequency. Modal damping is added by γ_1 and γ_2, but exact estimation of damping values lies outside the scope of this paper.

In our case, it happens that $\omega_1 \approx 2\omega_2$. Moreover, an optimal response is obtained if $\Omega = \omega_1$, and we shall assume that $\Omega \approx \omega_1$. Actually, when considering Hopf bifurcations in Section 3, in order to simplify the argument we shall assume that $\Omega = \omega_1$.

Before analyzing the equations of motion, we show a typical simulation result (Fig. 3), where the parameters are such that the stability of the trivial solution is lost. The trivial solution implies a certain amplitude for the directly driven mode of vibration and a zero amplitude for the bending mode of vibration. The directions of vibration are in principle perpendicular to each other. The direct driving force does not have a component in the bending direction. As the stability of the trivial solution of steady states is lost, the system settles in a different oscillatory mode, where both amplitudes are nonvanishing.

In the case of interest, we write $G = \varepsilon g$, $d_i = \varepsilon\delta_i$, $\gamma_i = \varepsilon\mu_i$, where ε is of order 0.1 and the other parameters are at most of unit order. As mentioned before, $\Omega \approx \omega_1 \approx 2\omega_2$. With the notation $\omega_1^2 - \Omega^2 = \chi_1\varepsilon$, $\omega_2^2 - \frac{\Omega^2}{4} = \chi_2\varepsilon$, the problem may be written as

$$\ddot{x}_1 + \Omega^2 x_1 = \varepsilon(g\cos(\Omega t) - \chi_1 x_1 - \delta_1 x_2^2 - \mu_1\dot{x}_1), \tag{13}$$

$$\ddot{x}_2 + \frac{\Omega^2}{4}x_2 = -\varepsilon(\delta_2 x_1 x_2 + \chi_2 x_2 + \mu_2\dot{x}_2 + \delta_3 x_2^3). \tag{14}$$

Writing

$$y_1 = x_1, \qquad y_2 = -\frac{\dot{x}_1}{\Omega}, \qquad y_3 = x_2, \qquad y_4 = -\frac{2\dot{x}_2}{\Omega},$$

we obtain the system

$$\dot{y} = Ay + \varepsilon f(y, t), \tag{15}$$

where

$$A = \begin{pmatrix}0 & -\Omega & 0 & 0\\ \Omega & 0 & 0 & 0\\ 0 & 0 & 0 & -\frac{\Omega}{2}\\ 0 & 0 & \frac{\Omega}{2} & 0\end{pmatrix} \quad \text{and}$$

$$f(y,t) = \begin{pmatrix}0\\ -\frac{1}{\Omega}[g\cos(\Omega t) - \chi_1 y_1 - \delta_1 y_3^2 + \mu_1\Omega y_2]\\ 0\\ \frac{2}{\Omega}\left[\delta_2 y_1 y_3 + \chi_2 y_3 - \frac{\mu_2\Omega}{2}y_4 + \delta_3 y_3^3\right]\end{pmatrix}.$$

With $u := e^{-At}y$, we have the system

$$\dot{u} = \varepsilon e^{-At}f(e^{At}u),$$

which is periodic in t, with period $T = \frac{4\pi}{\Omega}$. In order to make the analysis tractable, we shall from now on study the averaged system. For details concerning the procedure of averaging, the reader is referred to [13].

Setting $u := (u_1, v_1, u_2, v_2)^T$, we obtain

$$\begin{pmatrix}y_1\\ y_2\end{pmatrix} = \begin{pmatrix}u_1\cos(\Omega t) - v_1\sin(\Omega t)\\ u_1\sin(\Omega t) + v_1\cos(\Omega t)\end{pmatrix};$$

$$\begin{pmatrix}y_3\\ y_4\end{pmatrix} = \begin{pmatrix}u_2\cos\left(\frac{\Omega t}{2}\right) - v_2\sin\left(\frac{\Omega t}{2}\right)\\ u_2\sin\left(\frac{\Omega t}{2}\right) + v_2\cos\left(\frac{\Omega t}{2}\right)\end{pmatrix}.$$

Please cite this article in press as: C. van der Avoort, et al., Parametric resonance and Hopf bifurcation analysis for a MEMS resonator, Physica D (2011), doi:10.1016/j.physd.2011.01.004

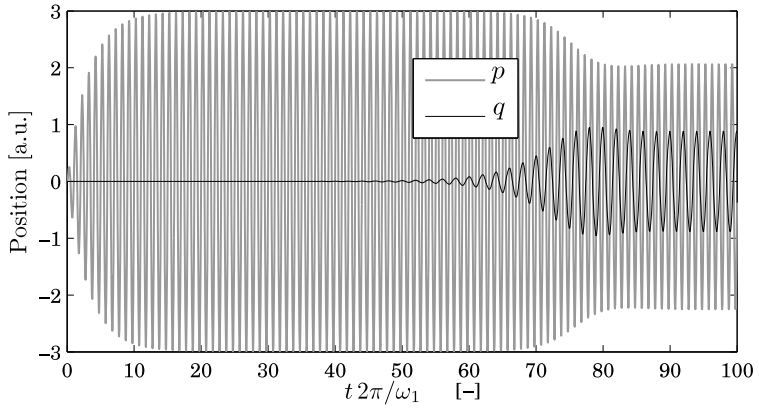

Fig. 3. Integration of the system in Eq. (10), when $\omega_1 = 2\omega_2$, $\Omega = \omega_1 = 1$, $G = 0.3$ and $\gamma_1 = \gamma_2 = 0.1$, $d_1 = 0.25$, $d_2 = 0.05$, $d_3 = 0$.

Note that a constant u represents a periodic orbit for the original system (15). A simple computation yields the equation in Box I and the averaged equations read

$$\dot{\bar{u}}_1 = \frac{-\varepsilon}{2\Omega}(\chi_1\bar{v}_1 + \mu_1\Omega\bar{u}_1 + \delta_1\bar{u}_2\bar{v}_2), \tag{16}$$

$$\dot{\bar{v}}_1 = \frac{-\varepsilon}{2\Omega}\left(g - \chi_1\bar{u}_1 + \mu_1\Omega\bar{v}_1 - \delta_1\frac{\bar{u}_2^2 - \bar{v}_2^2}{2}\right), \tag{17}$$

$$\begin{aligned}\dot{\bar{u}}_2 \;=\; & -\frac{\varepsilon}{\Omega}\left(\chi_2\bar{v}_2 + \frac{\mu_2\Omega}{2}\bar{u}_2 + \frac{3\delta_3}{4}(\bar{v}_2^3 + \bar{u}_2^2\bar{v}_2)\right.\\ & \left.-\frac{\delta_2(\bar{u}_1\bar{v}_2 - \bar{u}_2\bar{v}_1)}{2}\right),\end{aligned} \tag{18}$$

$$\begin{aligned}\dot{\bar{v}}_2 \;=\; & \frac{\varepsilon}{\Omega}\left(\chi_2\bar{u}_2 - \frac{\mu_2\Omega}{2}\bar{v}_2 + \frac{3\delta_3}{4}(\bar{u}_2^3 + \bar{u}_2\bar{v}_2^2)\right.\\ & \left.+\frac{\delta_2(\bar{u}_1\bar{u}_2 + \bar{v}_1\bar{v}_2)}{2}\right).\end{aligned} \tag{19}$$

For determining the steady states of this system, it turns out to be advantageous to introduce the new unknown variables

$$z_1 := \bar{u}_1 + i\bar{v}_1; \qquad z_2 := \bar{u}_2 + i\bar{v}_2;$$
$$z_3 := \bar{u}_2 - i\bar{v}_2; \qquad z_4 := \bar{u}_1 - i\bar{v}_1.$$

We rescale time in order to get rid of the factor $\frac{\varepsilon}{2\Omega}$. The Eqs. (16)–(19) in this setting read

$$\dot{z}_1 = -ig + (-\mu_1\Omega + i\chi_1)z_1 + \frac{\delta_1 i z_2^2}{2}, \tag{20}$$

$$\dot{z}_2 = (-\mu_2\Omega + 2i\chi_2)z_2 + \delta_2 i z_1 z_3 + \frac{3\delta_3 i z_2^2 z_3}{2}, \tag{21}$$

$$\dot{z}_3 = -(\mu_2\Omega + 2i\chi_2)z_3 - \delta_2 i z_4 z_2 - \frac{3\delta_3 i z_3^2 z_2}{2}, \tag{22}$$

$$\dot{z}_4 = ig - (\mu_1\Omega + i\chi_1)z_4 - \frac{\delta_1 i z_3^2}{2}. \tag{23}$$

By $Z_1, \ldots, Z_4$ we denote any steady state of this system. Obviously,

$$-ig + (-\mu_1\Omega + i\chi_1)Z_1 + \frac{\delta_1 i Z_2^2}{2} = 0, \tag{24}$$

$$(-\mu_2\Omega + 2i\chi_2)Z_2 + \delta_2 i Z_1 Z_3 + \frac{3\delta_3 i Z_2^2 Z_3}{2} = 0, \tag{25}$$

$$-(\mu_2\Omega + 2i\chi_2)Z_3 - \delta_2 i Z_4 Z_2 - \frac{3\delta_3 i Z_3^2 Z_2}{2} = 0, \tag{26}$$

$$ig - (\mu_1\Omega + i\chi_1)Z_4 - \frac{\delta_1 i Z_3^2}{2} = 0. \tag{27}$$

We shall write $R_1^2 := Z_1 Z_4$; $R_2^2 = Z_2 Z_3$. Writing $Z_1 = U_1 + iV_1$, $Z_2 = U_2 + iV_2$, $Z_3 = U_2 - iV_2$ and $Z_4 = U_1 - iV_1$, we see that $R_1^2 = U_1^2 + V_1^2$, $R_2^2 = U_2^2 + V_2^2$. A situation where $R_2 = 0$ represents an in-plane situation, which we call trivial and which corresponds to in-plane oscillations of the bar. For such a situation,

$$\tilde{Z}_1 = g\frac{\chi_1 - i\mu_1\Omega}{\chi_1^2 + \mu_1^2\Omega^2}; \qquad \tilde{Z}_4 = \overline{\tilde{Z}_1}.$$

We interpret the clipping phenomenon, as described in Section 1, as the appearance of a new stable branch of solutions (namely: out-of-plane oscillations), whereby the trivial steady state loses its stability. We shall now compute the nontrivial steady states where $R_2 \neq 0$. To do that, we use (24) to express Z_1 in Z_2, and then plug the result into (25):

$$\begin{aligned}&(-\mu_2\Omega + 2i\chi_2)Z_2 - \frac{\delta_2 g}{-\mu_1\Omega + i\chi_1}Z_3\\ &\quad + \frac{\delta_1\delta_2 R_2^2 Z_2}{2(-\mu_1\Omega + i\chi_1)} + \frac{3}{2}\delta_3 i R_2^2 Z_2 = 0.\end{aligned} \tag{28}$$

Similarly, expressing Z_4 in Z_3 from (27) and putting it into (26), yields

$$\begin{aligned}&(-\mu_2\Omega - 2i\chi_2)Z_3 - \frac{\delta_2 g}{-\mu_1\Omega - i\chi_1}Z_2\\ &\quad + \frac{\delta_1\delta_2 R_2^2 Z_3}{2(-\mu_1\Omega - i\chi_1)} - \frac{3}{2}\delta_3 i R_2^2 Z_3 = 0.\end{aligned} \tag{29}$$

Considering R_2 fixed for the moment, these equations constitute a linear system in Z_2, Z_3; the existence of nontrivial solutions requires the determinant to vanish. That is,

$$\begin{aligned}&\left(1 - \frac{6\chi_1\delta_3}{\delta_1\delta_2} + \frac{9\delta_3^2(\chi_1^2 + \mu_1^2\Omega^2)}{\delta_1^2\delta_2^2}\right)R_2^4\\ &\quad + \left(\frac{4}{\delta_1\delta_2}(\mu_1\mu_2\Omega^2 - 2\chi_1\chi_2) + \frac{24\chi_2\delta_3(\chi_1^2 + \mu_1^2\Omega^2)}{\delta_1^2\delta_2^2}\right)R_2^2\\ &\quad + \frac{4\mu_2^2\Omega^2 + 16\chi_2^2}{\delta_1^2\delta_2^2}(\chi_1^2 + \mu_1^2\Omega^2) - 4\frac{g^2}{\delta_1^2} = 0.\end{aligned} \tag{30}$$

And conversely, if R_2 satisfies (30) then, obviously, the system (28), (29) admits a solution with the property that $|Z_2 Z_3| = R_2^2$. Writing

$$Z_2 = R_2 e^{i\Phi_2}, \qquad Z_3 = R_2 e^{-i\Phi_2},$$

a simple computation yields that Φ_2 satisfies

$$\begin{aligned}&\mu_1\mu_2\Omega^2 - 2\chi_1\chi_2 + \frac{(\delta_1\delta_2 - 3\delta_3\chi_1)R_2^2}{2} - i\left(\mu_2\Omega\chi_1 + 2\mu_1\Omega\chi_2\right.\\ &\quad \left.+ \frac{3}{2}\delta_3\mu_1\Omega R_2^2\right) = \delta_2 g e^{-2i\Phi_2}.\end{aligned} \tag{31}$$

Please cite this article in press as: C. van der Avoort, et al., Parametric resonance and Hopf bifurcation analysis for a MEMS resonator, Physica D (2011), doi:10.1016/j.physd.2011.01.004

$$f(e^{At}u) = \begin{pmatrix} 0 \\ -\frac{1}{\Omega}\left[\cos(\Omega t)\left(g - \chi_1 u_1 + \mu_1\Omega v_1 - \delta_1\frac{u_2^2 - v_2^2}{2}\right) + \sin(\Omega t)(\chi_1 v_1 + \mu_1\Omega u_1 + \delta_1 u_2 v_2) - \delta_1\frac{u_2^2 + v_2^2}{2}\right] \\ 0 \\ \frac{2}{\Omega}\left[\cos\left(\frac{\Omega t}{2}\right)\left(\chi_2 u_2 - \frac{\mu_2\Omega}{2}v_2 + \delta_3\frac{u_2^3 + 3u_2v_2^2}{2}\right) - \sin\left(\frac{\Omega t}{2}\right)\left(\chi_2 v_2 + \frac{\mu_2\Omega}{2}u_2 + \delta_3\frac{v_2^3 + 3u_2^2v_2}{2}\right)\right. \\ \quad + \cos(\Omega t)\cos\left(\frac{\Omega t}{2}\right)\left(\delta_2 u_1 u_2 + \delta_3\frac{u_2^3 - 3u_2v_2^2}{2}\right) + \sin(\Omega t)\sin\left(\frac{\Omega t}{2}\right)\delta_2 v_1 v_2 \\ \left.\quad + \cos(\Omega t)\sin\left(\frac{\Omega t}{2}\right)\left(\delta_3\frac{v_2^3 - 3u_2^2v_2}{2} - \delta_2 u_1 v_2\right) - \sin(\Omega t)\cos\left(\frac{\Omega t}{2}\right)\delta_2 v_1 u_2\right] \end{pmatrix}$$

Box I.

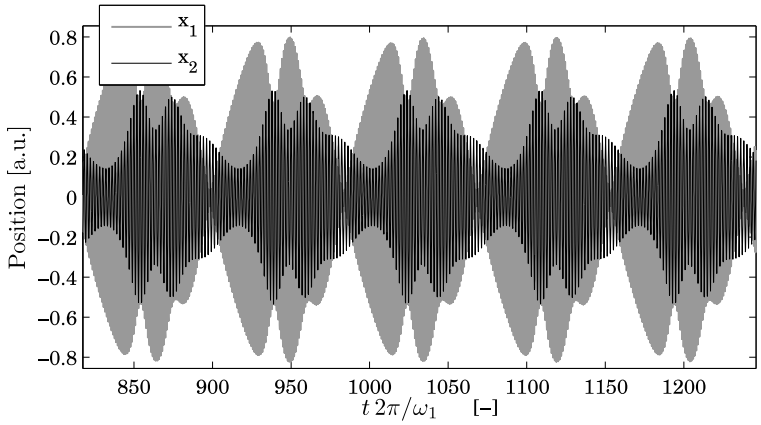

Fig. 4. Numerical integration of the system in Eqs. (13) and (14). The result shows a repeating pattern of vibrations in which energy is exchanged between the modes continuously.

It is now simple to compute Z_2 and Z_3. Note that Z_1 and Z_4 may be computed from (25) and (26):

$$-\delta_2 i Z_1 = (-\mu_2\Omega + 2i\chi_2)\frac{Z_2}{Z_3} + \frac{3\delta_3 i Z_2^2}{2},$$

$$\delta_2 i Z_4 = -(\mu_2\Omega + 2i\chi_2)\frac{Z_3}{Z_2} - \frac{3\delta_3 i Z_3^2}{2}.$$

To obtain R_1, we multiply these two equations and use that $Z_1Z_4 = R_1^2$; $Z_2Z_3 = R_2^2$:

$$\delta_2^2 R_1^2 = \mu_2^2\Omega^2 + 4\chi_2^2 + \frac{9}{4}\delta_3^2 R_2^4 + 6\delta_3\chi_2 R_2^2. \tag{32}$$

Substituting $R_2 = 0$ in (30) yields a value g^*, which is easily seen to be critical in the following sense: *when $g < g^*$, the trivial steady state is asymptotically stable, while for $g > g^*$ it is unstable. When $g = g^*$, $R_2 = 0$ and R_1 and R_2 satisfy (32), the nontrivial steady state branches off.* The stability of the nontrivial steady state is the subject of the next section.

3. The occurrence of beating: Hopf bifurcations

Experimental evidence clearly shows beating phenomena under appropriate conditions, and beating is also observed in simulations of the full system (10), see Fig. 4.

We shall show that, at appropriate non-trivial steady states (that is: $R_2 \neq 0$), the averaged system is susceptible to Hopf bifurcations, which seems to explain the aforementioned beating phenomena. In order to simplify the computations further, we assume from now on that

$$\chi_1 = 0, \mu_1 > 0 \quad \text{and} \quad \mu_2 > 0. \tag{33}$$

Actually, this is in accordance with the practical situation.

Let $Z = (Z_1, Z_2, Z_3, Z_4)$ be a steady state, that is, a solution of (24)–(27). Given (33), the matrix of the linearization around Z reads (see Box II). Using (32), the fact that $Z_1Z_4 = R_1^2$, $Z_2Z_3 = R_2^2$ and (25) and (26), we obtain for A the characteristic equation

$$((\mu_1\Omega + \lambda)(\mu_2\Omega + \lambda + \theta) + \delta_1\delta_2 R_2^2)((\mu_1\Omega + \lambda) \times (\mu_2\Omega + \lambda - \theta) + \delta_1\delta_2 R_2^2) = 0, \tag{34}$$

where

$$\theta^2 = \mu_2^2\Omega^2 - 12\delta_3\chi_2 R_2^2 - 9\delta_3^2 R_2^4. \tag{35}$$

(Note that $\theta \in \mathbb{C}$.) The next step is to identify situations where (34) has a pair of purely imaginary roots. First, we claim that, *in situations where (34) has purely imaginary roots, $\theta^2 > 0$.*

Indeed, in cases where $\theta = 0$, (34) essentially reduces to

$$\lambda^2 + (\mu_1 + \mu_2)\Omega\lambda + \mu_1\mu_2\Omega^2 + \delta_1\delta_2 R_2^2 = 0.$$

Purely imaginary roots imply that $\mu_1 + \mu_2 = 0$, which is not the case.

When $\theta^2 = -b^2$ and $\lambda = -ai$, with $a, b \in \mathbb{R}$, then without loss of generality we have

$$(\mu_1\Omega - ai)(\mu_2\Omega - (b + a)i) + \delta_1\delta_2 R_2^2 = 0.$$

Therefore,

$$\mu_1\mu_2\Omega^2 - a(a + b) + \delta_1\delta_2 R_2^2 = 0,$$
$$\mu_2 a + \mu_1(a + b) = 0$$

and

$$\mu_1\mu_2\Omega^2 + \frac{\mu_2}{\mu_1}a^2 + \delta_1\delta_2 R_2^2 = 0,$$

a contradiction, which proves the claim. So, in order that purely imaginary roots do exist, we must have that

$$\theta^2 > 0, \tag{36}$$

Please cite this article in press as: C. van der Avoort, et al., Parametric resonance and Hopf bifurcation analysis for a MEMS resonator, Physica D (2011), doi:10.1016/j.physd.2011.01.004

$$A = \begin{pmatrix} -\mu_1\Omega & i\delta_1 Z_2 & 0 & 0 \\ i\delta_2 Z_3 & -\mu_2\Omega + 2i\chi_2 + 3i\delta_3 Z_2 Z_3 & i\delta_2 Z_1 + \dfrac{3i\delta_3 Z_2^2}{2} & 0 \\ 0 & -i\delta_2 Z_4 - \dfrac{3i\delta_3 Z_3^2}{2} & -\mu_2\Omega - 2i\chi_2 - 3i\delta_3 Z_2 Z_3 & -i\delta_2 Z_2 \\ 0 & 0 & -i\delta_1 Z_3 & -\mu_1\Omega \end{pmatrix}$$

Box II.

which we shall assume from now on. In particular, this implies that each factor of the characteristic polynomial has real coefficients, and if λ is a purely imaginary root of such a factor, than $-\lambda$ is the second root. Without loss of generality we have

$$\lambda^2 + ((\mu_1+\mu_2)\Omega - \theta)\lambda + \mu_1\Omega(\mu_2\Omega - \theta) + \delta_1\delta_2 R_2^2 = 0, \quad (37)$$

which implies that

$$\theta = (\mu_1+\mu_2)\Omega. \quad (38)$$

This in turn implies that (37) reads

$$\lambda^2 - \mu_1^2\Omega^2 + \delta_1\delta_2 R_2^2 = 0. \quad (39)$$

This implies an additional necessary condition for the existence of purely imaginary eigenvalues:

$$\delta_1\delta_2 R_2^2 > \mu_1^2\Omega^2. \quad (40)$$

Note that (38) implies (36) and that (35) and (38) imply that

$$(\mu_1^2 + 2\mu_1\mu_2)\Omega^2 + 12\delta_3\chi_2 R_2^2 + 9\delta_3^2 R_2^4 = 0. \quad (41)$$

On the other hand, suppose that (41) holds true. Then $\theta^2 = \mu_2^2\Omega^2 - 12\delta_3\chi_2 R_2^2 - 9\delta_3^2 R_2^4 = (\mu_1+\mu_2)^2\Omega^2$, so that we may assume (38). Thus, we have established

Theorem 3.1. *In a steady state situation, the matrix of the linearization admits a pair of purely imaginary eigenvalues if and only if (41) and (40) are satisfied.*

Note that R_2 must be positive and, since δ_3 is positive, that $\chi_2 < 0$ in order that beating phenomena may be observed. This is in accordance with experimental evidence.

Taking into account that $\chi_1 = 0$, recall that the equation for the steady-state R_2 reads

$$\left(1 + \frac{9\delta_3^2\mu_1^2\Omega^2}{\delta_1^2\delta_2^2}\right) R_2^4 + \left(\frac{4\mu_1\mu_2\Omega^2}{\delta_1\delta_2} + \frac{24\chi_2\delta_3\mu_1^2\Omega^2}{\delta_1^2\delta_2^2}\right) R_2^2 + \frac{4\mu_2^2\Omega^2 + 16\chi_2^2}{\delta_1^2\delta_2^2}\mu_1^2\Omega^2 - 4\frac{g^2}{\delta_1^2} = 0. \quad (42)$$

When all other parameters are kept fixed, (42) defines a curve Γ in the (upper half) (g^2, R_2^2)-plane, germinating at $(g^{*2}, 0)$, where

$$g^{*2} = \frac{(\mu_2^2\Omega^2 + 4\chi_2^2)\mu_1^2\Omega^2}{\delta_2^2}.$$

Note that (42) may alternatively be written as

$$\left(R_2^2 + \frac{2\mu_1\mu_2\Omega^2}{\delta_1\delta_2}\right)^2 + \frac{\mu_1^2\Omega^2}{\delta_1^2\delta_2^2}(3\delta_3 R_2^2 + 4\chi_2)^2 = 4\frac{g^2}{\delta_1^2},$$

which implies that g^2 remains strictly positive along Γ. Clearly, Γ is a parabola. The strict positivity of g^2 implies that Γ cannot have a turning point at values $g^2 > g^{*2}$. This leaves us with two possibilities for the shape of Γ, vs. (see Fig. 5).

Type 1: Γ has a turning point to the left of g^{*2}, and

Type 2: Γ does not have a turning point.

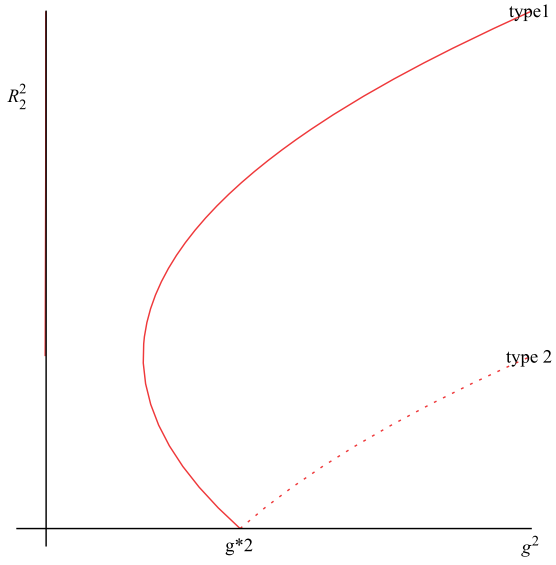

Fig. 5. Curves Γ for various values of χ_2 and μ_2.

Actually, depending on the values of the parameters, both possibilities actually occur. See Fig. 5. We remark that, when $g^2 < g^{*2}$, the trivial (in-plane-oscillation-) solution is stable, whereas the negative-slope part of Γ in the type 1 case represents an unstable situation. Once $g^2 > g^{*2}$, the trivial solution is unstable. In the previous section, we have seen that the the nontrivial solution is susceptible to Hopf bifurcations. Actually, a Hopf bifurcation can only occur in a point where Γ has positive slope, that is, $h(R_2^2) > 0$, where

$$h(R_2^2) := \frac{d(g^2)}{d(R_2^2)} = \frac{\delta_1^2}{2}\left\{\left(1 + \frac{9\delta_3^2\mu_1^2\Omega^2}{\delta_1^2\delta_2^2}\right) R_2^2 + \frac{2\mu_1\mu_2\Omega^2}{\delta_1\delta_2} + \frac{12\chi_2\delta_3\mu_1^2\Omega^2}{\delta_1^2\delta_2^2}\right\}.$$

This may be seen as follows. By (41),

$$12\delta_3\chi_2 = -\frac{(\mu_1^2 + 2\mu_1\mu_2)\Omega^2}{R_2^2} - 9\delta_3^2 R^2. \quad (43)$$

Inserting this value in the formula for h yields

$$h(R_2^2) = \frac{\delta_1^2}{2}\left(R_2^2 + \frac{2\mu_1\mu_2\Omega^2}{\delta_1\delta_2} - \frac{(\mu_1^2 + 2\mu_1\mu_2)\Omega^2}{R_2^2}\frac{\mu_1^2\Omega^2}{\delta_1^2\delta^2}\right).$$

By (40),

$$R_2^2 > \frac{\mu_1^2\Omega^2}{\delta_1\delta_2}, \quad \text{which implies that}$$

$$h(R_2^2) \geq \frac{\delta_1^2}{2}\left\{R_2^2 + \frac{2\mu_1\mu_2\Omega^2}{\delta_1\delta_2} - \frac{(\mu_1^2 + 2\mu_1\mu_2)\Omega^2}{\delta_1\delta_2}\right\} > 0.$$

By (40), the occurrence of a Hopf bifurcation implies that $\delta_1\delta_2 R_2^2 > \mu_1^2\Omega^2$. Writing $R_2^* := \frac{\mu_1\Omega}{\sqrt{\delta_1\delta_2}}$, choosing $R_2 = R_2^*$ and choosing χ_2

such that (41) is satisfied, if we plug these values for R_2^2 and χ_2 into (42), we find a (positive) value for g^2 which turns out to be strictly smaller than g^{*2}. Indeed, by (41),

$$\delta_1\delta_2\left(\left(1+\frac{9\delta_3^2\mu_1^2\Omega^2}{\delta_1^2\delta_2^2}\right)\frac{\mu_1^2\Omega^2}{\delta_1\delta_2}+\frac{4\mu_1\mu_2\Omega^2}{\delta_1\delta_2}+\frac{24\chi_2\delta_3\mu_1^2\Omega^2}{\delta_1^2\delta_2^2}\right)$$
$$=12\chi_2\delta_3R_2^2+2\mu_1\mu_2\Omega^2<0.$$

In this situation, we again have (43). This implies that, for this value of χ_2, $h(R_2^{*2})=0$: we are in a turning point of Γ, and therefore in a type 1 situation. If we now let R_2 grow a little bit, change χ_2 in such a way that (41) remains satisfied, and compute g according to (42), then we are necessarily in a situation where (34) has a pair of purely imaginary roots, and this happens at a g-value smaller than the corresponding (χ_2-dependent) value for g^*.

Let us now choose R_2^2 formally as a bifurcation parameter for the Hopf bifurcation, whereby it is understood that g^2 and χ_2 are chosen accordingly. It is then clear that

1. The critical value $R_2^{*2}:=\frac{\mu_1^2\Omega^2}{\delta_1\delta_2}$ can be seen as the onset of Hopf bifurcations.
2. The "onset point" $(\tilde{g}^2, R_2^{*2})$ is a turning point of Γ, and $\tilde{g}^2<g^{*2}$.
3. For any $R_2^2>R_2^{*2}$, χ_2 and g^2 can be chosen in such a way that we are in a Hopf bifurcation situation (the other parameters should be left fixed).

Finally, we show that Hopf bifurcations may also occur when Γ has no turning points:

Claim. *Choose δ_1, δ_2, μ_1 and μ_2 fixed, and choose $\delta_3\chi_2$ such that $\delta_1\delta_2\mu_2+6\chi_2\delta_3\mu_1=0$, that is, $h(0)=0$. For appropriate values of δ_3 and χ_2 ($\delta_3\chi_2$ fixed!), Γ contains a point where (34) has a pair of purely imaginary roots.*

Indeed, Eq. (41) now reads

$$(\mu_1^2+2\mu_1\mu_2)\Omega^2-2\frac{\delta_1\delta_2\mu_2}{\mu_1}R_2^2+9\delta_3^2R_2^4=0.$$

It admits a solution

$$R_2^2=\frac{\delta_1\delta_2\mu_2+\sqrt{\delta_1^2\delta_2^2\mu_2^2-9\delta_3^2(\mu_1^4+2\mu_1^3\mu_2)\Omega^2}}{9\mu_1\delta_3^2}.$$

Clearly, R_2^2 can be made arbitrarily large (and therefore $>\frac{\mu_1^2\Omega^2}{\delta_1\delta_2}$) by choosing δ_3 sufficiently small, and keeping fixed $\delta_3\chi_2$ and the remaining parameters. By (42), it is obvious that an appropriate value for g^2 exists.

It is rather obvious that a pair of purely imaginary roots for (34) implies the occurrence of a Hopf bifurcation if, say, g or χ_2 are varied. In order to find out whether the Hopf bifurcation is *supercritical or subcritical*, we must find the flow in the center manifold at a Hopf bifurcation point. In the previous arguments, the complex notation turned out to be computationally advantageous. For the present purpose, the original form of the system: (16)–(19) turns out to be computationally more tractable. Let U_1, V_1, U_2, V_2 represent a Hopf bifurcation situation, and let (by abuse of notation) A be the matrix of the corresponding linearization. Using Cayley–Hamilton and the decomposition (34), we set

$$P_1:=A^2+2(\mu_1+\mu_2)\Omega A+(\mu_1\Omega(\mu_1\Omega+2\mu_2\Omega)+\delta_1\delta_2R_2^2)I_4,$$
$$Q_1:=A^2+(\delta_1\delta_2R_2^2-\mu_1^2\Omega^2)I_4,$$

where I_4 is the 4×4 identity matrix and where we have used (38). Note that P_1 and Q_1 are both rank 2 matrices, commuting with A and each other, that $P_1Q_1=0$, and that P_1-Q_1 has rank 4. Setting

$$P:=(P_1-Q_1)^{-1}P_1;\qquad Q:=-(P_1-Q_1)^{-1}Q_1,$$

we again have that P and Q are both of rank 2, commute with each other and with A, $PQ=0$ and, finally, $P+Q=I_4$. In the present setting, P and Q have rather tractable forms (we have found this after computing them), which is the main reason for returning to U_1, V_1, U_2, V_2. P is a projection on the invariant subspace, generated by appropriate linear combinations of the eigenvectors, belonging to the purely imaginary eigenvalues; Q projects on the remaining invariant subspace. Let $i\omega$ be a purely imaginary eigenvalue (for the value of ω, see (39)), and let $0\neq e_1\in Im(P)$; choose $e_2=-\frac{Ae_1}{\omega}$ and choose $e_3, e_4\in Im(Q)$ in such a way that $\{e_1,\ldots,e_4\}$ is a basis of $\mathbb{R}^4$. Now write an orbit in the center manifold as $\mathbf{w}(t)=w_1(t)e_1+\cdots+w_4(t)e_4$, where $w_3=w_3(w_1,w_2)$, $w_4=w_4(w_1,w_2)$, $|w_3|+|w_4|=O(w_1^2+w_2^2)$. Using Maple, we were able to compute the Taylor expansion to order three of the flow, and to compute the first Lyapunov coefficient. The formal expressions were too complicated to print, even in Maple output. But for specific parameter values, the first Lyapunov coefficient can be computed without any problems. In all cases we found it to be negative, indicating that **the Hopf bifurcation is supercritical**.

4. Conclusions

The response of a MEMS resonator, driven in an in-plane length-extensional mode of excitation, may show unwanted clipping or beating phenomena. We have constructed a model, in which two different response modes (say: in-plane and out-of plane) have been incorporated, and we have shown that the unwanted phenomena can be ascribed to energy exchange between the modes (clipping) and a Hopf bifurcation (beating). New experimental evidence seems to imply that still more response modes must be incorporated in order to obtain a sufficiently precise description. It is clear that any extended model must be expected to exhibit stability and bifurcation aspects, similar to the model, studied in the present paper.

Acknowledgements

We thank Kim Le Phan for sharing the Polytec vibrometer measurement data in Fig. 2, and Jan A. Sanders for very helpful discussions.

References

[1] C.T.C. Nguyen, MEMS technology for timing and frequency control, IEEE Trans. Ultrason., Ferroelect., Freq. Contr. 54 (2007) 251–270.
[2] J.T.M. van Beek, K.L. Phan, G.J.A. Verheijden, G.E.J. Koops, C. van der Avoort, J. van Wingerden, D.E. Badaroglu, J.J.M. Bontemps, R. Puers, A piezo-resistive resonant MEMS amplifier, in: Proc. Int. Electr. Dev. Meeting, IEDM 2008, 2008, pp. 667–670.
[3] C. van der Avoort, et al., Amplitude saturation of MEMS resonators explained by autoparametric resonance, J. Mmech. Meng. 20 (2010) 105012.
[4] K.L. Turner, S.A. Miller, P.G. Hartwell, N.C. MacDonald, S.H. Strogatz, S.G. Adams, Five parametric resonances in a microelectromechanical system, Nature 396 (1998) 149–152.
[5] M. Zalalutdinov, A. Zehnder, A. Olkhovets, S. Turner, L. Sekaric, B. Ilic, D. Czaplewski, J.M. Parpia, H.G. Craighead, Auto-parametric optical drive for micromechanical oscillators, Appl. Phys. Lett. 79 (5) (2001).
[6] A. Vyas, D. Peroulis, A.K. Bajaj, Dynamics of a nonlinear microresonator based on resonantly interacting flexural–torsional modes, Nonlinear Dynam. 54 (2008) 31–52.
[7] F. Weidenhammer, Der eingespannte, achsial pulsierend belastete Stab als Stabilitätsproblem, Ing.-Arch. 19 (3) (1951) 162–191.
[8] T. Iwatsubo, Y. Sugiyama, S. Ogino, Simple and combination resonances of columns under periodic axial loads, J. Sound Vib. 33 (2) (1974) 211–221.
[9] M.P. Cartmell, J.W. Roberts, Simultaneous combination resonances in an autoparametrically resonant system, J. Sound Vib. 123 (1988) 81–101.
[10] A.H. Nayfeh, D.T. Mook, Parametric excitations of linear systems having many degrees of freedom, J. Acoust. Soc. Am. 62 (1977) 375–381.
[11] L. Meirovitch, Elements of Vibration Analysis, McGraw-Hill, 1986.
[12] L.H. Donnell, Beams, Plates and Shells, McGraw-Hill, 1976.
[13] J.A. Sanders, F. Verhulst, J. Murdock, Averaging Methods in Nonlinear Dynamical Systems, Springer, ISBN 978-0-387-48916-2, 2007.

Please cite this article in press as: C. van der Avoort, et al., Parametric resonance and Hopf bifurcation analysis for a MEMS resonator, Physica D (2011), doi:10.1016/j.physd.2011.01.004